

## Piezofluorochromic properties of AIE-active 9,10-bis(*N*-alkylpheno-thiazin-3-yl-vinyl-2)anthracenes with different length of alkyl chains

Meng Zheng, Mingxiao Sun, Yiping Li, Jianfeng Wang, Lingyu Bu, Shanfeng Xue, Wenjun Yang\*

Key Laboratory of Rubber-Plastics of Ministry of Education/Shandong Province (QUST), School of Polymer Science & Engineering, Qingdao University of Science & Technology, 53-Zhengzhou Road, Qingdao 266042, China



### ARTICLE INFO

#### Article history:

Received 5 August 2013

Received in revised form

1 October 2013

Accepted 9 October 2013

Available online 29 October 2013

#### Keywords:

9,10-Bis(*N*-alkylpheno-thiazin-3-yl-vinyl-2)anthracenes

Piezofluorochromism

Aggregation-induced emission

*N*-alkyl length-dependency

Wittig–Horner reaction

End group effect

### ABSTRACT

9,10-Bis(*N*-alkylpheno-thiazin-3-yl-vinyl-2)anthracenes (**PT-Cn**) with different carbon numbers (*n*) of alkyl chains (*n* = 2, 3, 5, 6, 7, 9, 12, 18) are prepared to further understand the effect of alkyl lengths on the solid-state fluorescence and piezochromic luminescence of alkyl-containing 9,10-bis(arylvinyl)anthracenes. The results show that the fluorescence emissions of both pressed and annealed **PT-Cn** are gradually blue-shifted, but the blue-shifted amplitudes of annealed states are more remarkable with the increase of alkyl length, leading to that longer alkyl-containing **PT-Cn** show larger piezofluorochromism (PFC) spectral shifts. Powder wide-angle X-ray diffraction and differential scanning calorimetry experiments reveal that the transformation between crystalline and amorphous states under various external stimuli is responsible for the PFC and restoration behaviors. This work demonstrates once again that combining the simple alternation of molecular chemical structure and the physical change of aggregate morphology under external stimuli could tune the solid-state optical properties of some organic fluorophores.

© 2013 Elsevier Ltd. All rights reserved.

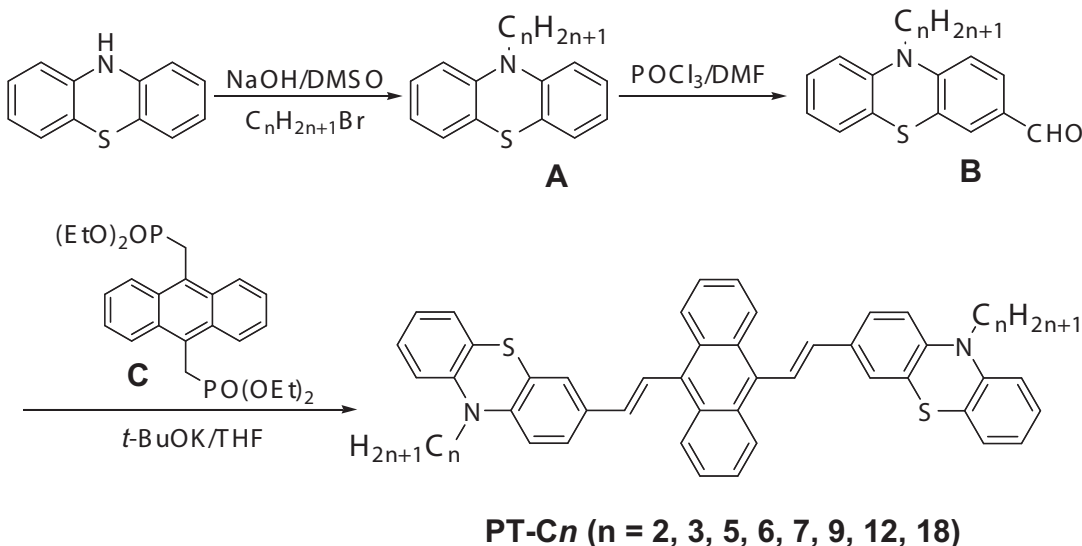
### 1. Introduction

Conjugated organic molecules exhibiting strong solid-state fluorescence are promising optical and optoelectronic materials, and tuning and switching the solid-state luminescence by external mechanical stimuli (such as grinding, pressing, shearing, deformation, etc. named mechano- or piezo-fluorochromism (PFC)), instead of the chemical alteration of molecular structures not only have potential applications in chemo- and mechano-sensors, data storage, security inks and optoelectronic devices but also profit the understanding of solid-state photophysical properties [1–8]. Recent studies have demonstrated that conjugated molecules with strongly twisted skeleton conformations not only show aggregation-induced/crystallization-enhanced emission but also are mostly promising candidates for PFC materials [8–26]. In this context, 9,10-bis(arylvinyl)anthracene derivatives have been the mainstay of PFC materials reported to date [17,23–32]. Interestingly, recent several reports show that PFC behaviors of some alkyl-

containing conjugated molecules are alkyl length-dependent, such as 9,10-bis(*p*-alkoxystyryl)anthracenes only with sufficient long alkyl chains (*n* ≥ 10, *n* represents carbon number of alkyl chains) are effective PFC materials [29], and 9,10-bis[(*N*-alkylcarbazol-3-yl)vinyl]- and 9,10-bis[(9,9-dialkyl-fluorene-2-yl)vinyl]anthracenes exhibit different alkyl length-dependent PFC behaviors [24,28], etc. These results not only underline the complexity of the structure–property relationship of PFC materials but also indicate the significant effect of the nature of end-aryl and substituents at the aryl rings on the solid-state fluorescence and piezochromic luminescence. 9,10-bis(*N*-alkylpheno-thiazin-3-yl-vinyl-2)anthracenes are also alkyl-containing 9,10-bis(arylvinyl)anthracene derivatives, and one of them, 9,10-bis(*N*-hexylpheno-thiazin-3-yl-vinyl-2)anthracene has been found to show remarkable PFC behavior [33]. To further understand the effect of alkyl chains on the solid-state fluorescence and piezochromic luminescence, in the current work, we have prepared a series of 9,10-bis(*N*-alkylpheno-thiazin-3-yl-vinyl-2)anthracenes (**PT-Cn**) with different length of alkyl chains (*n* = 2, 3, 5, 6, 7, 9, 12, 18, **Scheme 1**) and their fluorescence properties are investigated. We now report that the solid-state fluorescence emissions and PFC spectral shifts of **PT-Cn** are indeed related to the length of alkyl chains.

\* Corresponding author. Tel.: +86 532 84023670; fax: +86 532 84023977.

E-mail address: [ywjjph2004@qust.edu.cn](mailto:ywjjph2004@qust.edu.cn) (W. Yang).

**Scheme 1.** Synthetic route and structure of **PT-C<sub>n</sub>**.

## 2. Experimental section

### 2.1. Reagents and solvents

All the starting chemicals were purchased from Aldrich Chemical Co. Other solvents and reagents were analytical grade and used as received, unless otherwise stated. 9,10-bis(diethylphosphorylmethyl)anthracene was from previous work [34]. THF was distilled over metallic sodium and DMF over calcium hydride before use.

### 2.2. Measurement

<sup>1</sup>H and <sup>13</sup>C NMR spectra were recorded on a Bruker-AC500 spectrometer with CDCl<sub>3</sub> as solvent and teramethylsilane (TMS) as the internal standard. Elemental analysis was performed on Perkin–Elmer 2400. UV–vis absorption spectra were recorded on a Hitachi U-4100 spectrophotometer. Fluorescence measurements were carried out with Hitachi F-4600 spectrophotometer. The peak wavelength of the lowest energy absorption band was used as the excitation wavelength for the PL measurement. The fluorescence quantum yield ( $\phi$ ) was determined at room temperature by the dilution method using fluorescein in water (pH = 11) as the reference. Powder wide-angle X-ray diffraction (PXD) experiments were performed on a Powder X-ray Diffractometry (INCA Energy, Oxford Instruments) operating at 3 kW. Differential scanning calorimetry (DSC) curves were determined on a Netzsch DSC 204F1 at a heating rate of 10 °C/min.

### 2.3. Piezofluorochromic and stimulus-recovering experiments

Pressing experiment: A quantity of **PT-C<sub>n</sub>** and KBr powder was simply mixed in a mortar and then pressed with IR pellet press under the pressure of 1500 psi for 1 min at room temperature. Annealing experiment: The pressed sample (or molten solid) was put into an oven whose temperature was 40 °C over  $T_c$  (cold-crystallization temperature of each compound) for 2 min. Solvent-fuming experiment: The pressed sample was put above the dichloromethane level and exposed to the vapor for 1 min at room temperature. Grinding experiment: pristine solids were put on a glass plate and ground with a metal spatula at room temperature.

### 2.4. Synthesis

#### 2.4.1. 9,10-Bis(2-(10-hexylphenothiazin-3-yl)vinyl)anthracene (**PT-C7**)

9,10-Bis(diethylphosphorylmethyl)anthracene (0.10 g, 0.21 mmol) and 10-heptylphenothiazine-3-carbaldehyde (0.150 g, 0.46 mmol) was dissolved in anhydrous THF (20 mL). Potassium *tert*-butoxide (0.19 g, 1.67 mmol) was added and the suspension was stirred for 3 h at room temperature. Methanol was added into the mixture and a yellow-green solid was collected by filtration. The crude product was purified by silica gel column chromatography (petroleum ether/methylene chloride = 4:1, v/v). A yellowish-green solid with a yield of 75% (0.19 g) was obtained. <sup>1</sup>H NMR (500 MHz, CDCl<sub>3</sub>):  $\delta$  8.37 (q, 4H), 7.80 (s, 1H), 7.77 (s, 1H), 7.40–7.50 (m, 8H), 7.15–7.28 (m, 4H), 6.89–7.05 (m, 6H), 6.82 (s, 1H), 6.78 (s, 1H), 3.90 (t, 4H), 1.86 (qui, 4H), 1.29–1.56 (m, 16H), 0.89 ppm (t, 6H). <sup>13</sup>C NMR (125 MHz, CDCl<sub>3</sub>):  $\delta$  145.01, 136.19, 132.68, 131.91, 129.63, 127.49, 127.30, 126.47, 125.94, 125.38, 125.17, 124.99, 124.36, 123.42, 122.48, 115.40, 47.54, 31.92, 29.69, 29.36, 26.93, 22.62, 14.14 ppm. Anal. Calcd for C<sub>56</sub>H<sub>56</sub>N<sub>2</sub>S<sub>2</sub> (%): C, 81.91; H, 6.87; N, 3.41; S, 7.81. Found: C, 81.86; H, 6.91; N, 3.39; S, 7.85.

Other 9,10-bis(2-(10-alkylphenothiazin-3-yl)vinyl)anthracenes were synthesized as described for **PT-C7** except that different 10-alkylphenothiazine-3-carbaldehydes were used. After purification, they were characterized only by <sup>1</sup>H NMR because of their similar and simple structure. The <sup>1</sup>H NMR data were as follow:

#### 2.4.2. 9,10-Bis(2-(10-ethylphenothiazin-3-yl)vinyl)anthracene (**PT-C2**)

<sup>1</sup>H NMR (500 MHz, CDCl<sub>3</sub>)  $\delta$  8.36 (q, 4H), 7.80 (s, 1H), 7.76 (s, 1H), 7.40–7.49 (m, 8H), 7.16–7.27 (m, 4H), 6.89–7.03 (m, 6H), 6.82 (s, 1H), 6.78 (s, 1H), 3.86 (t, 4H), 0.98 ppm (t, 6H).

#### 2.4.3. 9,10-Bis(2-(10-propylphenothiazin-3-yl)vinyl)anthracene (**PT-C3**)

<sup>1</sup>H NMR (500 MHz, CDCl<sub>3</sub>)  $\delta$  8.37 (q, 4H), 7.81 (s, 1H), 7.75 (s, 1H), 7.40–7.49 (m, 8H), 7.16–7.26 (m, 4H), 6.89–7.02 (m, 6H), 6.82 (s, 1H), 6.78 (s, 1H), 3.85 (t, 4H), 1.86 (q, 4H), 0.90 ppm (t, 6H).

#### 2.4.4. 9,10-Bis(2-(10-pentylphenothiazin-3-yl)vinyl)anthracene (**PT-C5**)

<sup>1</sup>H NMR (500 MHz, CDCl<sub>3</sub>)  $\delta$  8.37 (q, 4H), 7.77 (s, 1H), 7.75 (s, 1H), 7.45–7.47 (m, 8H), 7.16–7.26 (m, 4H), 6.89–7.02 (m, 6H), 6.82

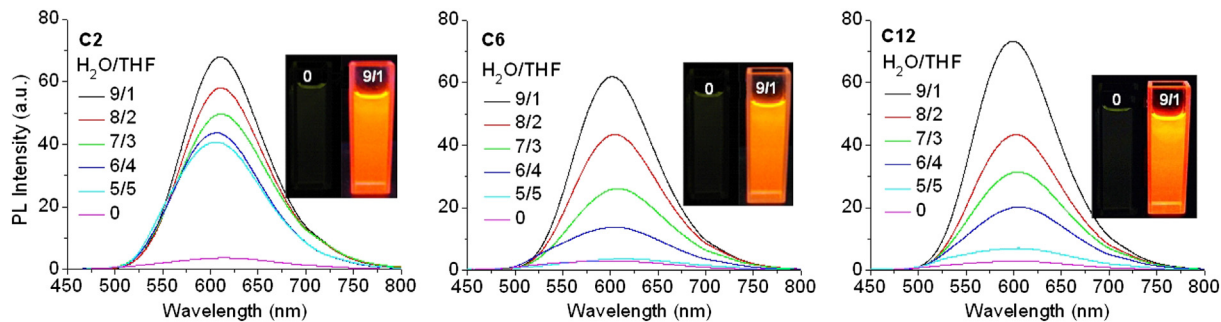


**Fig. 1.** Emission (PL) spectra of **PT-Cn** at  $1.0 \times 10^{-5}$  M in water–THF mixtures; the insets are the fluorescence images with water contents of 0% and 90% under illumination with a 365 nm UV lamp.

(s, 1H), 6.78 (s, 1H), 3.90 (t, 4H), 1.86 (q, 4H), 1.29–1.56 (m, 8H), 0.92 ppm (t, 6H).

#### 2.4.5. 9,10-Bis(2-(10-hexylphenothiazin-3-yl)vinyl)anthracene (**PT-C6**)

$^1\text{H}$  NMR (500 MHz,  $\text{CDCl}_3$ )  $\delta$  8.34 (q, 4H), 7.80 (s, 1H), 7.76 (s, 1H), 7.39–7.49 (m, 8H), 7.14–7.25 (m, 4H), 6.88–7.94 (m, 6H), 6.80 (s, 1H), 6.77 (s, 1H), 3.89 (t, 4H), 1.84 (q, 4H), 1.29–1.56 (m, 12H), 0.89 ppm (t, 6H).

#### 2.4.6. 9,10-Bis(2-(10-nonylphenothiazin-3-yl)vinyl)anthracene (**PT-C9**)

$^1\text{H}$  NMR (500 MHz,  $\text{CDCl}_3$ )  $\delta$  8.36 (q, 4H), 7.80 (s, 1H), 7.77 (s, 1H), 7.40–7.50 (m, 8H), 7.15–7.28 (m, 4H), 6.89–7.02 (m, 6H), 6.82 (s, 1H), 6.78 (s, 1H), 3.90 (t, 4H), 1.86 (q, 4H), 1.27–1.56 (m, 24H), 0.88 ppm (t, 6H).

#### 2.4.7. 9,10-Bis(2-(10-dodecylphenothiazin-3-yl)vinyl)anthracene (**PT-C12**)

$^1\text{H}$  NMR (500 MHz,  $\text{CDCl}_3$ )  $\delta$  8.36 (q, 4H), 7.80 (s, 1H), 7.77 (s, 1H), 7.40–7.50 (m, 8H), 7.16–7.27 (m, 4H), 6.89–6.95 (m, 6H), 6.82 (s, 1H), 6.79 (s, 1H), 3.90 (t, 4H), 1.85 (q, 4H), 1.26–1.56 (m, 36H), 0.88 ppm (t, 6H).

#### 2.4.8. 9,10-Bis(2-(10-octadecylphenothiazin-3-yl)vinyl)anthracene (**PT-C18**)

$^1\text{H}$  NMR (500 MHz,  $\text{CDCl}_3$ )  $\delta$  8.36 (q, 4H), 7.80 (s, 1H), 7.77 (s, 1H), 7.40–7.50 (m, 8H), 7.15–7.26 (m, 4H), 6.88–6.95 (m, 6H), 6.82 (s, 1H), 6.79 (s, 1H), 3.90 (t, 4H), 1.85 (q, 4H), 1.25–1.49 (m, 60H), 0.87 ppm (t, 6H).

### 3. Results and discussion

Synthetic route and structure of 9,10-bis(2-(10-octadecylphenothiazin-3-yl)vinyl)-anthracenes (**PT-Cn**) was depicted in Scheme 1. The alkylation of phenothiazine with different *n*-alkyl bromides followed by the treatment with  $\text{POCl}_3/\text{DMF}$  produced 10-alkyl-3-formylphenothiazines (**B**) with different length of alkyl chains [35]. The Wittig–Horner reaction of **B** and 9,10-bis(diethylphosphorylmethyl)anthracene (**C**) afforded the target compounds **PT-Cn** in good high yields (75–91%) [35]. The chemical composition and structure of these products were confirmed by proton nuclear magnetic resonance spectra and elemental analysis.

**PT-Cn** homologs are all highly soluble in common organic solvents, such as THF, chloroform, dichloromethane, and toluene. To understand whether these water-nonsoluble conjugated organic molecules are aggregation-induced emission (AIE) active, a large amount of water was added into the organic solution of the compound and the change of fluorescence intensity recorded (Fig. 1). In

contrast to the faint fluorescence of **PT-Cn** in THF, the aqueous dispersions of **PT-Cn** in THF–water mixtures at high water content exhibit strong fluorescence. Since water is the non-solvent for **PT-Cn**, the molecules of **PT-Cn** must have aggregated in THF–water mixtures with high water content. Therefore, **PT-Cn** homologs are strongly AIE-active. In addition, the aqueous dispersions of **PT-Cn** prepared by us emit bright orange fluorescence. Fig. 2 shows the fluorescence emission spectra of as-prepared (pristine) **PT-Cn** solids by evaporating the solvents (petroleum ether/methylene chloride). Among them, pristine **PT-C18** solid exhibits the most blue-shifted emission, and others are related irregularly to alkyl length.

The PFC and recovery behavior of **PT-Cn** (mixed with KBr to minimize the amount of fluorophores) is examined (Fig. 3). When they are pressed with an IR pellet press (30 s at 1500 psi), the pressed samples show red to orange colors from **PT-C2** to **PT-C18**. However, when the pressed samples are annealed before the isotropic melt transition or exposed to solvent vapor (fuming above dichloromethane), the fluorescence colors are changed into orange-yellow to green ones. Furthermore, when the fumed or annealed samples are re-pressed, the fluorescence colors are again changed as the first pressing. This process is reproducible, indicating a reversible PFC behavior. It is noted that **PT-Cn** with long alkyl chains exhibit more remarkable fluorescence color changes between pressed and annealed (or fumed) states.

Meanwhile, the emission spectra of above samples under various stimuli are recorded on a luminescence spectrophotometer (Fig. 4), and the corresponding peak emission wavelengths ( $\lambda$ ) are summarized in Table 1. It is shown that the emission spectra are very consistent with the corresponding fluorescence colors observed (Figs. 4 and 3). The  $\lambda_{\text{pressed}}$  and  $\lambda_{\text{annealed}}$  all decreased with the increase of alkyl length, and the decrease of  $\lambda_{\text{annealed}}$  is more obvious (Table 1). Although short alkyl (**C2**, **C3**, and **C5**) and middle

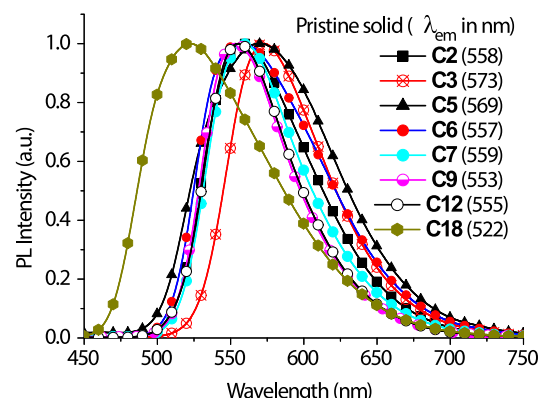


**Fig. 2.** Emission spectra pristine **PT-Cn** solids.

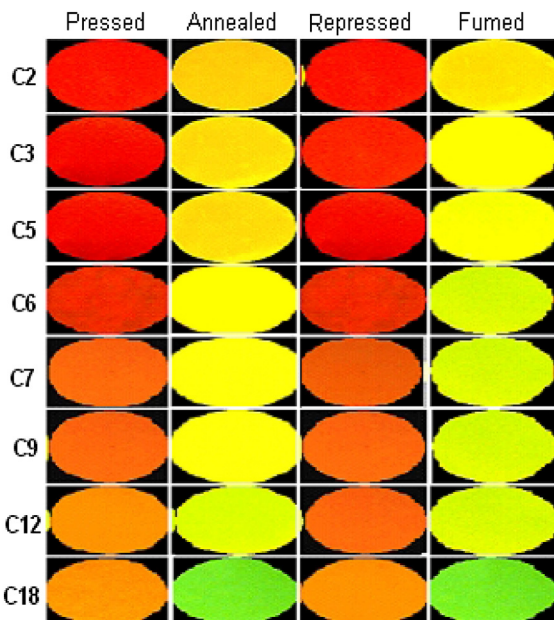


**Fig. 3.** Fluorescence images of **PT-Cn** mixed with KBr upon external stimuli under a 365 nm UV lamp.

**Table 1**  
Peak emission wavelengths ( $\lambda$ , in nm) of **PT-Cn** solids under various external stimuli.

<b>PT-Cn</b>	<b>C2</b>	<b>C3</b>	<b>C5</b>	<b>C6</b>	<b>C7</b>	<b>C9</b>	<b>C12</b>	<b>C18</b>
$\lambda_{\text{pressed}}$	620	608	607	605	600	599	595	588
$\lambda_{\text{annealed}}$	577	568	563	554	546	547	537	517
$\lambda_{\text{repressed}}$	621	614	608	605	604	600	601	593
$\lambda_{\text{fumed}}$	572	553	560	541	537	546	534	514
$\Delta\lambda_{\text{PFC}}^{\text{a}}$	43	40	44	51	54	52	58	71

<sup>a</sup>  $\Delta\lambda_{\text{PFC}} = \lambda_{\text{pressed}} - \lambda_{\text{annealed}}$ .

alkyl (**C6**, **C7**, and **C9**) **PT-Cn** show similar pressing-induced spectral shifts ( $\Delta\lambda_{\text{PFC}} = \lambda_{\text{pressed}} - \lambda_{\text{annealed}}$ ), respectively (**Table 1**), the general trend of  $\Delta\lambda_{\text{PFC}}$  increases with the length of alkyl chains. Therefore, **PT-Cn** homologs are also alkyl chain length-dependent PFC materials, and alkyl chains have played a functional role in tuning the PFC behavior. Without doubt, X-ray analysis of single crystals should give more accurate information. Unfortunately, the single crystals of long alkyl-containing **PT-Cn** such as **PT-C12** and **PT-C18** suitable for X-ray analysis are not obtained, and the origin for this alkyl chain length-dependent PFC behavior is not clear at present.

To gain an insight into the PFC behavior of **PT-Cn** solids, powder wide-angle X-ray diffraction (PWXD) and differential scanning calorimetry (DSC) experiments are conducted on the pristine and ground solids. As shown in **Fig. 5(a)**, pristine solids show sharp and intense reflections, indicative of the well-ordered microcrystalline structures. In contrast, the ground solids display

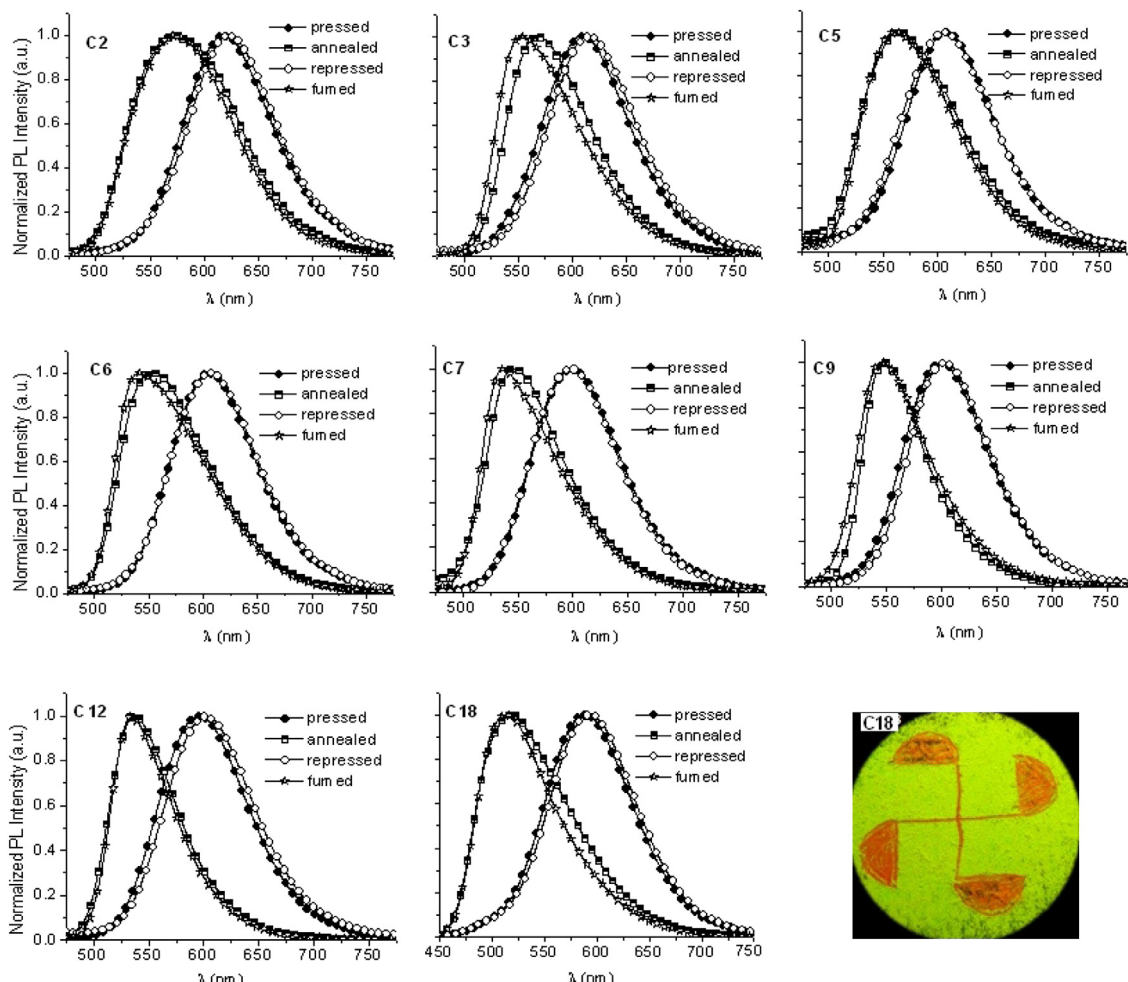


**Fig. 4.** Normalized emission spectra of **PT-Cn** mixed with KBr upon external stimuli and image of **TP-C18** casted on a filter paper and drawn a windmill with a metal spatula.

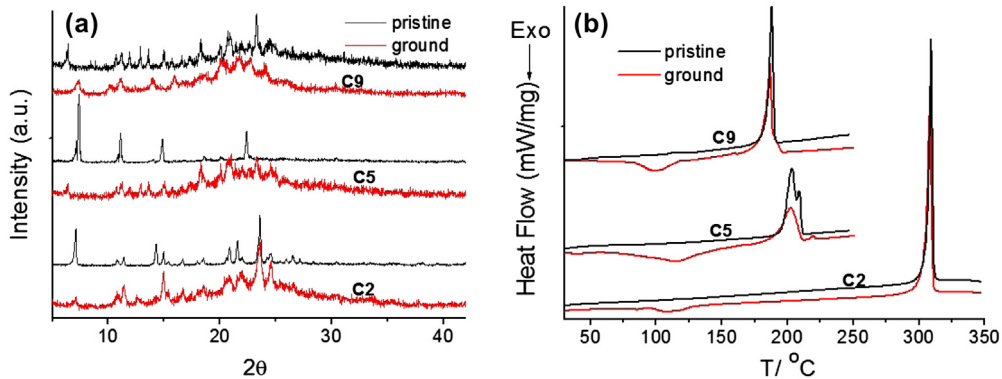


**Fig. 5.** Powder X-ray diffraction patterns at room temperature (a) and DSC curves (b) of pristine and ground **PT-Cn** solids.

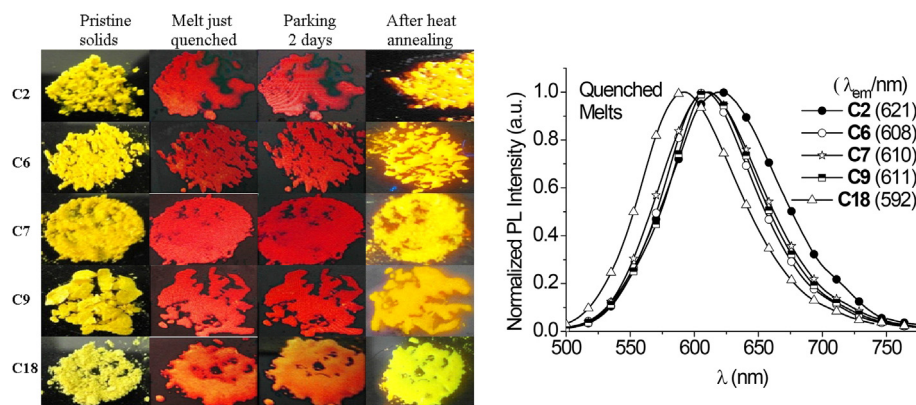


**Fig. 6.** Images of **PT-Cn** solids after melting and then annealing under illumination of 365 nm UV lamp (left) and normalized emission spectra under quenched melt states (right).

broad and featureless reflections along with a series of overlapped peaks reflecting notable amorphous features. Therefore, grinding has induced the phase transition of **PT-Cn** solids between crystalline and amorphous states, which should be responsible for their PFC behavior. This PFC mechanism could be confirmed by DSC experiments. Fig. 5(b) shows that no additional thermal transitions are detected for all pristine solids before the isotropic melt transition; however, there is clearly one exothermic transition peak at the lower-temperature region for respective ground solids. This broad exothermic peak could be ascribed to the cold-crystallization of amorphized **PT-Cn** solids upon heat annealing [24,28].

To further understand experimentally the contribution of amorphization–crystallization transition to the PFC behavior of **PT-Cn**, **PT-Cn** solids are melted and then quenched in liquid nitrogen, which could be considered to afford real amorphous solids. It is observed that both the just quenched and long-time parked melts at room temperature show similar fluorescence images and emission spectra (Fig. 6), which are also similar to those of pressed samples (*vide supra*). When the quenched melts are annealed before respective melt points, the blue-shifted fluorescence colors are observed, same as above pressed samples upon annealing. This finding evidences further that the transformation between crystalline and amorphous states upon various external stimuli is responsible for the PFC behavior of **PT-Cn**.

#### 4. Conclusions

We have synthesized a series of 9,10-bis(*N*-alkylphenothiazin-3-yl-vinyl-2)-anthracenes (**PT-Cn**) with different length of *N*-alkyl chains and investigated the optical properties. These aggregation-

induced emission homologs exhibit alkyl length-related piezo-fluorochromic (PFC) behavior whose PFC spectral shifts ( $\Delta\lambda_{PFC}$ ) increase with the extension of alkyl length. **PT-Cn** homologs become new alkyl chain length-dependent PFC materials, and a remarkable  $\Delta\lambda_{PFC}$  up to 71 nm for **PT-C18** is observed. PFC mechanism that the transformation between crystalline and amorphous states upon external stimuli is revealed by power X-ray diffraction and differential scanning calorimetry analysis and further evidenced by melt-crystallization experiment. This work demonstrates once again that subtle manipulation of end groups of 9,10-divinylanthracene derivatives could endow them with unique and tunable solid-state optical properties. The revelation of alkyl length-dependent PFC behavior is a challenging subject and is underway in our laboratory.

#### Acknowledgment

We thank the NSF of China (No. 51173092, 51073083, 51303091), NSF of Shandong Province and Qingdao City (No. ZR2010EM023, ZR2012EMQ003, 13-1-4-207-jch), and the Doctoral Found of QUST (No. 0022541).

#### References

- [1] Sagara Y, Kato T. Mechanically induced luminescence changes in molecular assemblies. *Nat Chem* 2009;1:605–10.
- [2] Weder Christoph. Mechanoresponsive materials [Editorial]. *J Mater Chem* 2011;21:8235–6.
- [3] Chi Z, Zhang X, Xu B, Zhou X, Ma C, Zhang Y, et al. Recent advances in organic mechanofluorochromic materials. *Chem Soc Rev* 2012;41:3878–96.
- [4] Luo J, Li L, Song Y, Pei J. A piezochromic luminescent complex: mechanical force induced patterning with a high contrast ratio. *Chem Eur J* 2011;17: 10515–9.

- [5] Crenshaw B, Burnworth M, Khariwala D, Hiltner A, Mather P, Simha R, et al. Deformation-induced color changes in mechanochromic polyethylene blends. *Macromolecules* 2007;40:2400–8.
- [6] Zhang X, Chi Z, Zhang Y, Liu S, Xu J. Recent advances in mechanochromic luminescent metal complexes. *J Mater Chem C* 2013;1:3376–90.
- [7] Taniguchi Y. Organic solid-state laser. *J Photopolym Sci Technol* 2002;15: 183–4.
- [8] Barbarella G, Melucci M, Sotgiu G. The versatile thiophene: an overview of recent research on thiophene-based materials. *Adv Mater* 2005;17:1581–93.
- [9] Zhao N, Yang Z, Lam J, Sung H, Xie N, Chen S, et al. Benzothiazolium-functionalized tetraphenylethene: an AIE luminogen with tunable solid-state emission. *Chem Commun* 2012;48:8637–9.
- [10] Zhao N, Li M, Yan Y, Lam J, Zhang Y, Zhao Y, et al. A tetraphenylethene-substituted pyridinium salt with multiple functionalities: synthesis, stimuli-responsive emission, optical waveguide and specific mitochondrion imaging. *J Mater Chem C* 2013;1:4640–6.
- [11] Zhang Y, Zhuang G, Ouyang M, Hu B, Song Q, Sun J, et al. Mechanochromic and thermochromic fluorescent properties of cyanostilbene derivatives. *Dyes Pigment* 2013;98:486–92.
- [12] Liang J, Hu F, Lv X, Chen Z, Chen Z, Yin J. Synthesis, characterization and mechanochromic behavior of binuclear gold(I) complexes with various diisocyanato bridges. *Dyes Pigment* 2012;95:485–90.
- [13] Sagara Y, Mutai T, Yoshikawa I, Araki K. Material design for piezochromic luminescence: hydrogen-bond-directed assemblies of a pyrene derivative. *J Am Chem Soc* 2007;129:1520–1.
- [14] Sagara Y, Yamane S, Mutai T, Araki K, Kato T. A stimuli-responsive, photoluminescent, anthracene-based liquid crystal: emission color determined by thermal and mechanical processes. *Adv Funct Mater* 2009;19:1869–75.
- [15] Zhang Z, Yao D, Zhou T, Zhang H, Wang Y. Reversible piezo- and photochromic behaviors accompanied by emission color switching of two anthracene-containing organic molecules. *Chem Commun* 2011;47:7782–4.
- [16] Li H, Chi Z, Xu B, Zhang X, Li X, Liu S, et al. Aggregation-induced emission enhancement compounds containing triphenylamine–anthrylenevinylene and tetraphenylethene moieties. *J Mater Chem* 2011;21:3760–7.
- [17] Dong Y, Xu B, Zhang J, Tan X, Wang L, Chen J, et al. Piezochromic luminescence based on the molecular aggregation of 9,10-bis((E)-2-(pyrid-2-yl)vinyl)anthracene. *Angew Chem Int Ed* 2012;51:10782–5.
- [18] Zhao Z, Liu J, Lam J, Chan C, Qiu H, Tang B. Luminescent aggregates of a starburst silole-triphenylamine adduct for sensitive explosive detection. *Dyes Pigment* 2011;91:258–63.
- [19] Zhang X, Chi Z, Xu B, Li H, Yang Z, Li X, et al. Synthesis of blue light emitting bis(triphenylethylene) derivatives: a case of aggregation-induced emission enhancement. *Dyes Pigment* 2011;89:56–62.
- [20] Wang Q, Liu H, Lu H, Xu Z, Lai G, Li Z, et al. Synthesis, characterization and solid-state emission properties of arylsilyl-substituted pyrene derivatives. *Dyes Pigment* 2013;99:771–8.
- [21] Yoon S, Park S. Polymorphic and mechanochromic luminescence modulation in the highly emissive dicyanodistyrylbenzene crystal: secondary bonding interaction in molecular stacking assembly. *J Mater Chem* 2011;21:8338–46.
- [22] Kei M, Hideyuki N. Mechanofluorochromism of 4-[bis(9,9-dimethylfluoren-2-yl)amino]benzaldehyde. *Dyes Pigment* 2013;96:76–80.
- [23] Yang Z, Chi Z, Xu B, Li H, Zhang X, Li X, et al. High- $T_g$  carbazole derivatives as a new class of aggregation-induced emission enhancement materials. *J Mater Chem* 2010;20:7352–9.
- [24] Wang Y, Liu W, Bu L, Li J, Zheng M, Zhang D, et al. Reversible piezochromic luminescence of 9,10-bis[(N-alkylcarbazol-3-yl)vinyl]anthracenes and the dependence on N-alkyl chain length. *J Mater Chem C* 2013;1:856–62.
- [25] Bu L, Li Y, Wang J, Sun M, Zheng M, Liu W, et al. Synthesis and piezochromic luminescence of aggregation-enhanced emission 9,10-bis(N-alkylcarbazol-2-yl-vinyl-2)anthracenes. *Dyes Pigment* 2013;99:833–8.
- [26] Liu W, Wang Y, Sun M, Zhang D, Zheng M, Yang W. Alkoxy-position effects on piezofluorochromism and aggregation-induced emission of 9,10-bis(alkoxystyryl)anthracenes. *Chem Comm* 2013;49:6042–4.
- [27] Li J, Liu T, Zheng M, Sun M, Zhang D, Zhang H, et al. Dibutylaminophenyl- and/or pyridinyl-capped 2,6,9,10-tetravinylanthracene cruciforms: synthesis and aggregation-enhanced one- and two-photon excited fluorescence. *J Phys Chem C* 2013;117:8404–10.
- [28] Bu L, Sun M, Zhang D, Liu W, Wang Y, Zheng M, et al. Solid-state fluorescence properties and reversible piezochromic luminescence of aggregation-induced emission-active 9,10-bis[(9,9-dialkylfluorene-2-yl)vinyl]anthracenes. *J Mater Chem C* 2013;1:2028–35.
- [29] Liu W, Wang Y, Bu L, Li J, Sun M, Zhang D, et al. Chain length-dependent piezofluorochromic behavior of 9,10-bis(p-alkoxystyryl)anthracenes. *J Lumin* 2013;143:50–5.
- [30] Schwaebel T, Trapp O, Bunz U. Digital photography for the analysis of fluorescence responses. *Chem Sci* 2013;4:273–81.
- [31] Kim S, Zheng Q, He G, Bharali D, Pudavar H, Baev A, et al. Aggregation-enhanced fluorescence and two-photon absorption in nanoaggregates of a 9,10-bis[4’-(4”-aminostyryl)styryl]anthracene derivative. *Adv Funct Mater* 2006;16:2317–23.
- [32] He J, Xu B, Chen F, Xia H, Li K, Ye L, et al. Aggregation-induced emission in the crystals of 9,10-distyrylanthracene derivatives: the essential role of restricted intramolecular torsion. *J Phys Chem C* 2009;113:9892–9.
- [33] Zhang X, Chi Z, Zhang J, Li H, Xu B, Li X, et al. Piezofluorochromic properties and mechanism of an aggregation-induced emission enhancement compound containing N-hexylphenoxythiazine and anthracene moieties. *J Phys Chem B* 2011;115(23):7606–11.
- [34] Zhang H, Guo E, Zhang Y, Ren P, Yang W. Donor–acceptor-substituted anthracene-centered cruciforms: synthesis, enhanced two-photon absorptions, and spatially separated frontier molecular orbitals. *Chem Mater* 2009;21:5125–35.
- [35] Lee S, Cho M, Yoon H, Lee S, Kim J, Zhang Q, et al. *Macromol Res* 2004;12:484–9.